IEEE Access
Multidisciplinary | Rapid Review | Open Access Journal

Received May 22, 2017, accepted June 9, 2017, date of publication June 13, 2017, date of current version July 31, 2017.

Digital Object Identifier 10.1109/ACCESS.2017.2715119

A Simple and Versatile Field Prediction Model for Indoor and Indoor-to-Outdoor Propagation

VITTORIO DEGLI-ESPOSTI[1], (Senior Member, IEEE), ENRICO M. VITUCCI[1], (Member, IEEE), AND R. MARTIN[2]

[1]Dipartimento di Ingegneria dell'Energia Elettrica e dell'Informazione "Guglielmo Marconi," Alma Mater Studiorum - University of Bologna, IT-40136 Bologna, Italy
[2]Polaris Wireless Inc., Mountain View, CA 94043, USA

Corresponding author: Vittorio Degli-Esposti (v.degliesposti@unibo.it)

This work was supported by a research collaboration Project between Polaris Wireless Inc. and the University of Bologna.

ABSTRACT A simple field prediction model based on a combination of a two-parameter propagation formula and a multi-wall model is proposed for fast and yet accurate indoor and indoor-to-outdoor field prediction. The model's approach is based on: 1) simplicity; 2) physical soundness; and 3) adaptability to the available environment-database format. The model is validated versus both ray tracing and measurements in different environments and it is shown to perform very well in all cases. Moreover, the model is very fast and can exploit the accuracy plus of deterministic prediction based on the 3-D indoor building map whenever it is available.

INDEX TERMS Indoor radio communication, radiowave propagation, propagation losses, UHF measurements, ray tracing, electromagnetic modeling.

I. INTRODUCTION

Urban mobile radio propagation models are traditionally subdivided into two distinct classes: outdoor models and indoor models. In the first case a large-scale approach is chosen where only the external shape and materials of buildings are considered relevant to the propagation process, which can take place over a relatively vast area, whereas in the second case the internal building structure and characteristics are taken into account but the model's prediction domain is usually limited to one building. Each of the two cases have specific, reference environment representation formats: clutter maps or ESRI shapefile building databases [1] are common for outdoor models, while 3D digital building maps (e.g. the Autocad DXF format [2]) are used for indoor studies. Physics does not acknowledge boundaries between such scenarios and most real-life applications would require dealing somehow with both of them. Unfortunately, combining a large scale approach with the level of detail required to properly model indoor propagation is difficult due to both the mixed-database handling problems and the high computational demand.

Some propagation studies have tried to bridge the gap addressing outdoor-to-indoor propagation [3]–[7], or indoor radio coverage from both indoor and outdoor transmitters using a holistic approach [8].

Only a few studies have addressed indoor-to-outdoor propagation: two of them dealt with empirical-statistical propagation modeling for system simulation, interference analysis and planning [9], [10], while a third one focused on site-specific prediction using a combination of a ray model and an indoor finite-difference prediction method [11]. A fourth study addressed semi-deterministic modeling for interference analysis in LTE femtocells [12].

In addition to the above mentioned applications, indoor to outdoor propagation can also be important to assist fingerprinting localization techniques based on signals coming from both outdoor and indoor cell sites or access points, which can achieve good accuracy in dense urban areas where other localization techniques (e.g. GPS) fail [13], [14]. In their classic implementation however, such applications require either extensive calibration measurements or, alternatively, fast and yet accurate site-specific propagation models to build the reference RF maps for a very large number of base station sites over vast domains encompassing indoor and outdoor areas. 3D Ray-based models or finite-difference methods, although accurate, are not compliant with such requirements due to the heavy computation involved. Multi-wall models that take into account transmission through walls along the radial path, initially proposed in [15] then modified and improved even in more recent times [16], [17], although can achieve good performance in terms of both speed and accuracy, miss important propagation phenomena such as guiding effects between floors in large buildings or attenuation due to clutter [18].

In the present work a fast and versatile field prediction model for both indoor and indoor-to-outdoor propagation that can adapt itself to different kinds of environment database formats - from simple clutter maps to 3D building maps - is presented. The model is based on an extended version of the Meaningful path-loss Formula (MF) presented in [18]. The MF model, although very simple, has been shown to take into account all major propagation processes and to provide a good accuracy tradeoff when the detailed map of the building is not available.

Here the MF model has been (a) modified to extend prediction to the urban area adjacent the considered building, and (b) combined with a Multi-Wall model that's automatically enabled whenever a digital building map is available. Due to (b) the new model is called Multi-Wall Meaningful Formula (MW-MF) in the rest of this paper.

The new MW-MF model is here validated vs. Ray Tracing (RT) and indoor measurements in the same environments considered in [18], and the performance improvement achievable thanks to the knowledge of the internal building structure is assessed. Moreover, the model is shown to perform almost as well as RT in a reference environment, and this finding is briefly discussed in section III. Additionally, the MW-MF model is also tested in an indoor-to-outdoor case with good results.

The MW-MF model is thus shown to be a useful tool for fast and yet accurate field-strength prediction in indoor and near-indoor areas, with flexible interfacing with different real-world environment databases.

II. THE DESCRIPTION OF THE MODEL

The MW-MF field prediction model described here is an evolution of the MF model presented in [18]. The rationale of the model is still based on taking into account the two major indoor propagation processes, i.e. guiding effects and obstruction due to walls or cluttering using a variable path-loss exponent α, and a specific-attenuation parameter β, respectively. In addition to that, the model has been modified to allow systematic prediction in the building where the transmitter is located (the Tx building in the following) and in the urban area around it, until a specified distance or maximum Path Loss (PL), and to self-adapt to the available building database formats.

More specifically, the 2 major changes described below have been introduced.

First of all the model has been generalized to take into account multiple indoor/outdoor transitions and extend prediction outside of the considered Tx building. In order to achieve that we introduced transition distances d_i, transition losses L_i and different values of α and β (α_i, β_i), so that PL at distance d from the Tx can be expressed as:

$$PL\ [dB] = PL\ (d_{i-1}) + L_{i-1} + 10\alpha_i \log\left(\frac{d}{d_{i-1}}\right) + \beta_i\ (d - d_{i-1}) \quad \text{for } d_{i-1} < d \le d_i \tag{1}$$

The model still performs prediction along radials Tx-Rx. Based on a "building mask" clutter-map indicating whether each pixel is indoor or outdoor, the model detects indoor/outdoor transitions based on pixel-value changes along the radial, adds a given average transition loss L_{i-1} at distance d_{i-1} and then varies parameters α_i and β_i depending on whether the i-th radial section is indoor or outdoor, as shown in Fig. 1. Free-space parameter values are chosen for outdoor radial-sections ($\alpha = 2$, $\beta = 0$), but a non-null value for β can be considered to account for vegetation attenuation.

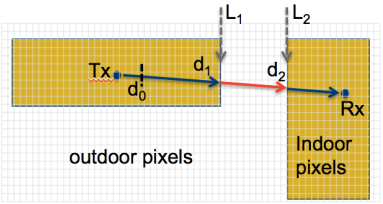

FIGURE 1. Radial path with different transition distances and radial sections over a building-mask database (2D view).

Of course prediction must be limited to a small area around the Tx building, where the radial path with a few outdoor/indoor transitions is dominant. Since indoor cell sites and access points are anyway conceived to serve only indoor areas and minimize outdoor coverage spill-over, this limitation should not be an issue in practice.

Note that, since no obstacles are usually present in the first meters along the radial line and guiding effects (if any) also settle in after a given distance, the first transition d_0 simply corresponds to the transition between free space propagation ($\alpha = 2$, $\beta = 0$) and propagation with the chosen parameter values (α_1, β_1) for the considered building, and not to a physical indoor/outdoor transition, thus $L_0 = 0$.

In case the Tx and the Rx are on different floors, an additional vertical attenuation PL^v is added to formula 1 with expression:

$$PL^v\ [dB] = \beta_i^v \left(d^v - d_{i-1}^v\right) \tag{2}$$

where d^v and d_{i-1}^v are distances projected along the vertical direction and β_1^v is the corresponding additional specific attenuation [dB/m] accounting for attenuation through floors. In particular β_1^v is equal to zero for outdoor sections, and is equal to the average floor attenuation divided by distance between floors for indoor sections.

The second major change with respect to the MF model consists in the "blending" of a multi-wall attenuation engine similar to [15] into the model: site-specific, average wall or floor penetration attenuations along each radial are taken into account and summed to PL expression (1) for each pixel when an indoor map for the Tx building is available. The MW-MF engine checks whether the indoor transmitter falls within the convex hull of an available building map. If so, radial-path intersections with walls and floors present in the map are searched and corresponding penetration losses taken

into account. Consequently the specific attenuations β_1 and β_1^v for the Tx building are reduced (e.g. down to 0.1 [dB/m]) because they don't have to account for wall/floor attenuation anymore but only for clutter attenuation. For the time being, the "multi-wall mode" can only be activated in the Tx building, but extension to nearby buildings having an available map is straightforward. In this case, transition losses L_i in (1) should be disabled, of course.

A general flow-chart of the algorithm explaining the flexible handling of the input format is shown in Fig. 2.

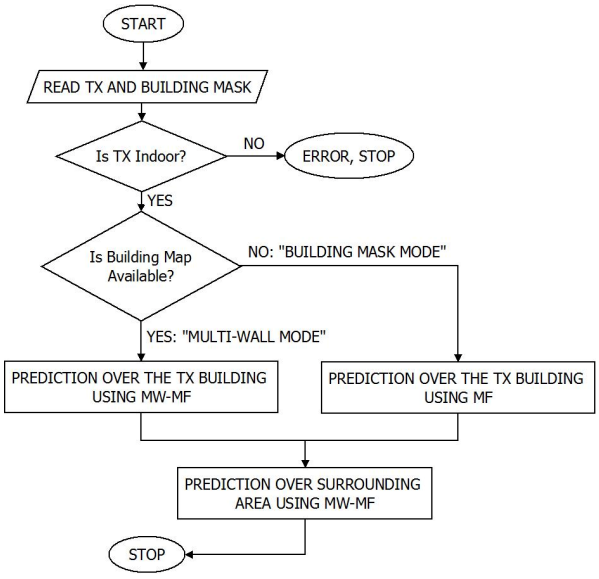

FIGURE 2. General flow-chart of the MW-MF algorithm.

Typical values for α and β are the same as for the MF model when no building map is available, i.e. in "building mask mode". Reference values for transition losses L_i can be found in the literature, where outdoor-to-indoor penetration has been widely studied [3]–[7]. Typically 7 dB for residential (wooden) buildings and glass-and-steel buildings and 10 dB for brick/concrete buildings should be used at UHF frequencies.

We would like to point out that transition losses as well as indoor wall attenuations must be set to average, empirically-determined values in order to take into account the effect of openings such as windows and doors and of multiple reflections inside different material layers on the overall transmission loss.

III. COMPARISON WITH RT IN AN IDEALIZED ENVIRONMENT

The large ideal environment representative of a shopping mall or airport wing considered in [18] is the first benchmark for assessing MW-MF performance in multi-wall mode, and also assessing the improvement margin over MF prediction already performed in [18], which for a single building is equivalent to MW-MF prediction in building-mask mode. Validation vs. RT is carried out over the whole floor-plan of the building on a 2.5m step grid with 1539 Rx points, or "pixels."

As in [18], the reference RT model is the full-3D model described in [19], used with a maximum of 3 successive reflections, 21 through-wall transmissions, 1 diffraction and 1 diffuse scattering. Diffuse scattering is modeled through the Effective Roughness model [19], using a single-lobe scattering pattern and S = 0.4. Dielectric parameters used in RT simulation are: ($\varepsilon_r = 5, \sigma = 0.002$) for concrete external walls, ($\varepsilon_r = 5, \sigma = 1$) for reinforced-concrete floor and ceiling, ($\varepsilon_r = 1.5, \sigma = 0.002$) for gypsum-board partitioning walls, where ε_r is the relative electric permittivity and σ is the conductivity [S/m]. Partitioning wall's parameters are chosen to generate a penetration loss of about 3 dB, as considered in [18].

MW-MF prediction is performed using $\alpha = 1.2$ (found to give best results in [18]) while β is set to zero since wall attenuation is already taken into account by the multi-wall algorithm while cluttering is of course absent in this ideal case.

RT prediction, MW-MF prediction and the prediction error of the latter with respect to RT are shown in Figures 3, 4 and 5, respectively, for a Distributed Antenna System (DAS) configuration with two simultaneous transmitters ($P_t = 0$ dBm, $f = 1935$ MHz) located at coordinates (170,20) and (190,20) with half-wavelength dipole antennas at all radio terminals.

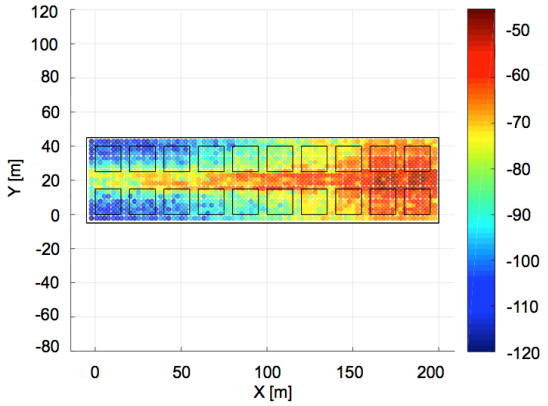

FIGURE 3. RT prediction (received power [dBm]) over the whole "ideal shopping mall" floorplan.

It is evident that MW-MF can predict wall obstructions and the corridor guiding effect almost as accurately as RT. The overall RMS error of MW-MF vs. RT is of 4.8 dB (mean error <E>= 0.6 dB, error standard deviation $\sigma_E = 4.7$ dB). Such a figure is 5 dB lower than what found in [18] using the MF model, where RMS error was of 9.9 dB, but of course the MF model doesn't need a site-specific map of building walls.

While RT, being a full-wave model that computes the coherent sum of each ray's field at each pixel, can predict the multipath fading ripple, MW-MF can't, and therefore the error plot has "speckles" (Fig. 5), which contribute to most of the RMS error mentioned above. In fact, the RMS

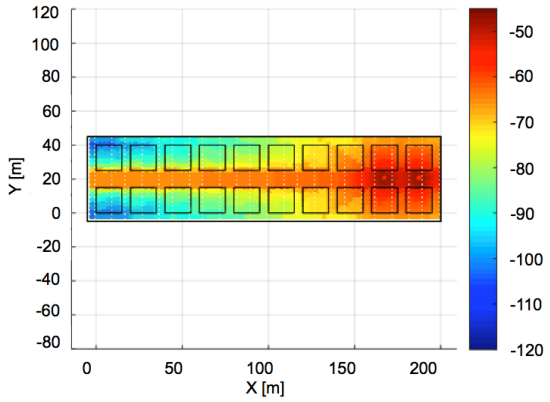

FIGURE 4. MW-MF prediction (received power [dBm]) over the whole "ideal shopping mall" floorplan.

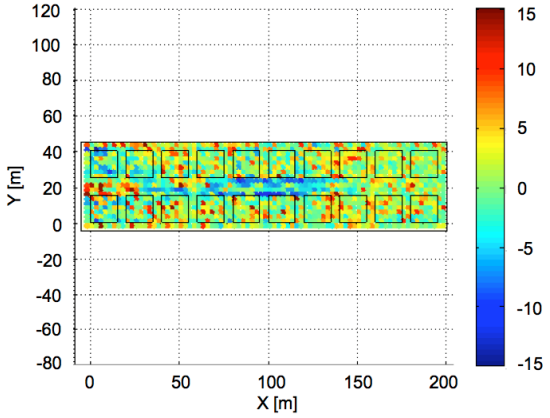

FIGURE 5. Error plot (MW-MF prediction minus RT prediction [dBm]) over the whole "ideal shopping mall" floorplan.

error of MW-MF vs. incoherent-mode RT - i.e. summing ray-powers instead of ray fields, not shown here for brevity – is of only 2 dB! Incoherent RT however misses important propagation mechanisms such as guiding effects that MW-MF can take into account through proper calibration of parameter α. Moreover, since RT-predicted fast-fading cannot be pin-point accurate in real-world applications due to small inaccuracies in the exact position and characteristics of each wall, RT prediction is likely to achieve similar error figures as MW-MF prediction when compared to actual measurements, but at a much higher computational cost.

In fact, irrespective of the number of bounces taken into account, RT was found to have an irreducible error standard deviation floor of about 5 dB in [20].

IV. PERFORMANCE IN REAL ENVIRONMENTS

The proposed MW-MF model has been validated vs. indoor measurements in the same two real environments considered in [18]. The first one is a typical office environment with gypsum-board dividing walls. The second environment is Villa Griffone, (Sasso Marconi, Italy), a 18th century mansion with thick, stone and brick walls where Guglielmo Marconi made his first radio telegraphy experiments. Detailed maps of the buildings and measurement routes can be found in [21] and [22], respectively. In addition to Tx locations considered in [22], some cases where Tx is 1 floor above the Rx are considered for Villa Griffone. Measurements have been done at 2 LTE frequencies (858 MHz and 1935 MHz), using omnidirectional antennas, an Agilent MXG Signal Generator, and an Agilent MXA signal analyzer. More details about the measurement set up can be found in [21]. Local averages over areas having a linear dimension of several wavelengths have been done at each Rx test point, in order to filter out the small-scale fading effects.

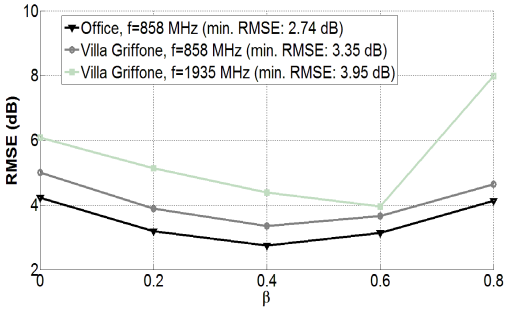

FIGURE 6. Best-fit β values for different environments and carrier's frequencies.

The model's parameter α is always set to 2 except for corridors cases where $\alpha = 1.7$ is used, exactly as in [18], while a simple optimization was carried out to find the best β value for the different cases, as shown in Fig. 6. The best-fit value $\beta = 0.4$ for the 858 MHz band is consistent with what found in [18] where it was slightly higher ($\beta = 0.5$) because it had to account for partitioning wall's losses too. The best-fit β value is surprisingly the same for the two environments, while it's slightly higher for the 1935 MHz band: given the increasing-with-frequency penetration loss of most materials, this seems a reasonable result.

Wall attenuation is supposed to be of 5.5 dB for the 34-cm thick dividing walls in Villa Griffone and 3 dB for gypsum-board partitions in the office building. Floor attenuation is set to a typical value of 8 dB. Such values where derived from literature survey.

In the office environment several links in the LTE 858 MHz band with different Tx locations and Rx routes are considered. Comparison between measured and predicted PL local averages for the different routes are shown in Fig. 7. In Fig. 8 results are reported on a log-log scale and compared with the MF curve found in [18]: RMS error is a surprisingly low 2.74 dB for the MW-MF model vs. 5.2 dB for the MF model.

In the Villa Griffone environment several links in both the 858 MHz and the 1935 MHz LTE bands with different Tx locations on two different floors are considered. Results for the two frequency bands with terminals on the same floor

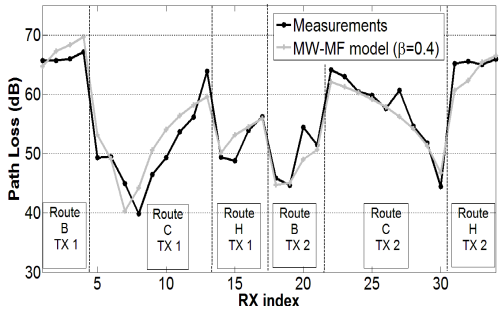

FIGURE 7. Measured vs. predicted PL for different Tx locations and RX routes in the office building at 858 MHz.

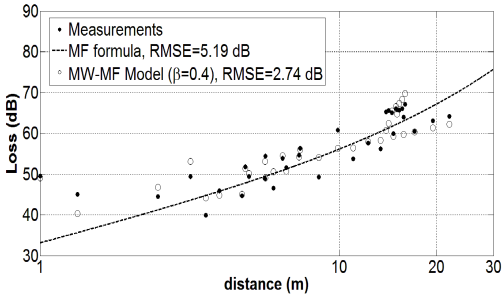

FIGURE 8. Measured and MW-MF predicted PL for the office building at 858 MHz, with MF best-fit curve.

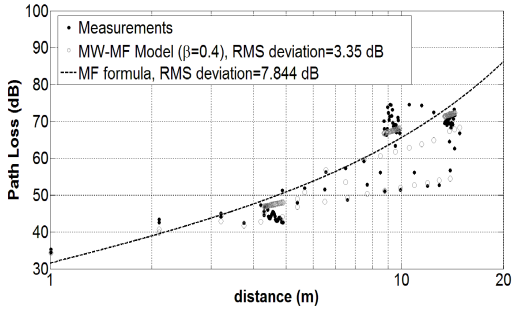

FIGURE 9. Measured and MW-MF-predicted PL for Villa Griffone at 858 MHz, with MF best-fit curve.

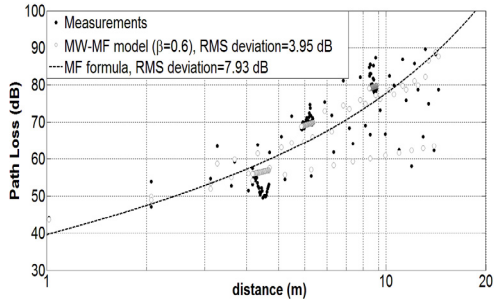

FIGURE 10. Measured and MW-MF predicted PL for Villa Griffone at 1935 MHz, with MF best-fit curve.

are shown on a log-log scale in Fig's. 9 and 10, respectively, where prediction results of the MF formula are also reported for reference.

Also here the MW-MF model shows a very good performance, with an RMS error of about 3-4 dB, 4 dB lower than with the MF model: the RMS error improvement obtainable by taking into account site-specific wall attenuation instead of considering a continuous specific attenuation (as in the MF model) is therefore confirmed to lie in the range 3 - 5 dB.

Results with Tx one floor above the Rx routes are shown in Fig's. 11 and 12, respectively. Even in this through-floor case, not considered in [18], the model performs very well with an RMS error of 4.8 and 2.7 dB in the 858 MHz and 1935 MHz cases, respectively.

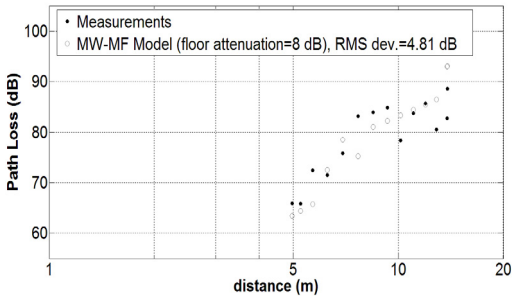

FIGURE 11. Measured and MW-MF predicted PL for Villa Griffone at 858 MHz, Tx is one floor above the Rx.

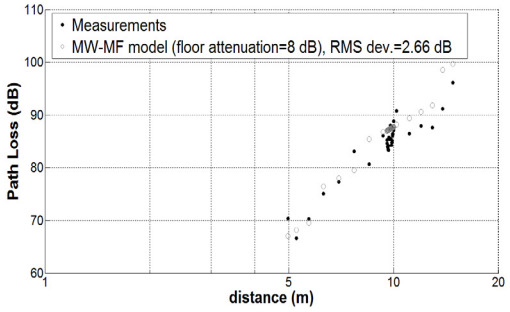

FIGURE 12. Measured and MW-MF predicted PL for Villa Griffone at 1935 MHz, Tx is one floor above the Rx.

Error statistics for the real environments are better than for the ideal shopping mall case: this is mostly due to the use of local-average measurements instead of punctual values.

The model has been validated vs. measurements also in indoor-to outdoor cases. It is not easy to find a proper environment for indoor-to-outdoor measurements because common-use indoor transmitters (e.g. WiFi access points) are often not powerful enough for the signal to be received from the streets around the building - if not from a few isolated spots - while ad-hoc, higher power transmitters would require explicit authorization from the competent Authority. In this paper we show results for a public mobile radio system cell-site that's installed inside the lobby of a big office building on California street, in central San Francisco. Cell site antenna is an omni-directional antenna, and radiated power is of 40 dBm. On the

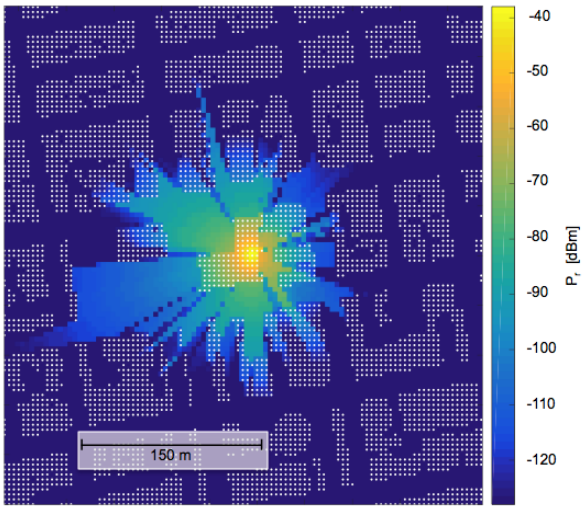

FIGURE 13. Building mask map and MW-MF prediction for the indoor cell site in central San Francisco.

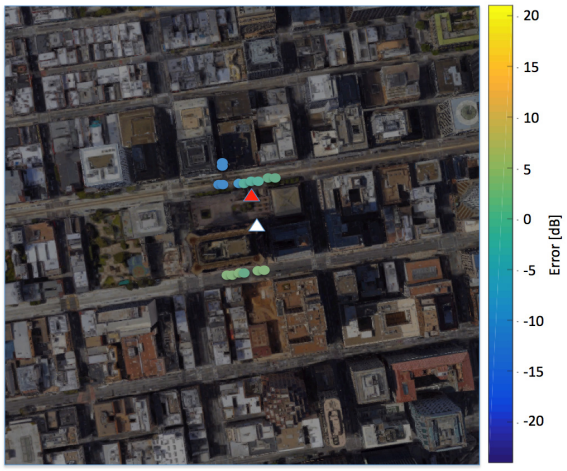

FIGURE 14. Prediction error in different Rx locations vs. locally averaged measured values for the indoor cell site in central San Francisco. Red triangle: original Tx position provided by the carrier; white triangle: modified Tx position (building block centroid).

receiver side, a Rhode-Schwarz scanner was placed in a minivan connected to a PCTEL OP178H omnidirectional antenna with 3 dBi gain that was placed on the minivan top at about 1.8m height. Exact Rx locations along measurement routes were tracked using a combination of GPS, inertial devices and speedometer. Using the scanner, the Received Signal Strength Indicator (RSSI) was recorded for the target broadcast control channels (BCCHs) as the minivan drove the streets around the cell site. Measurements yielded above-threshold RSSI values only along the two west-east streets next to the building complex.

Since no detailed map of the building was available, the MW-MF model was run in "building mask" mode using the same parameters used for the ideal shopping mall in [18], i.e. $\alpha = 1.2$, $\beta = 0.2$ [dB/m]. In addition, the indoor/outdoor transition loss was set to 7 dB since the building has mostly glass walls on the ground floor.

The original cell site location provided by the Cellular Carrier was a conventional location at the entrance of the complex on the north side of the block: using that location prediction error was very bad, with an RMS error of 26 dB. Moving the cell site in the center of the city block was enough to yield a very good RMS error of 4.6 dB ($<E>= 0.1$ dB, $\sigma_E = 4.5$ dB) without any parameter optimization! The corresponding predicted RSSI map is shown in Fig. 13. Computation time was of about 7 seconds on a single core of a 3.2 GHz Xeon CPU.

For reference, prediction error with respect to measurement local-averages is shown using color-scale dots over a satellite-view of the area in Fig. 14. There is a slight underestimation on the north side and a slight overestimation on the south side of the block, but overall prediction error is very low.

In Fig. 14 also the original Tx position provided by the carrier (red triangle) and the modified Tx position (in the building block centroid, white triangle) are shown.

V. CONCLUSIONS

An indoor and indoor-to-outdoor field prediction model has been developed on the base of the meaningful path-loss formula introduced in [18]. The model retains the formula's advantages, i.e. physical soundness and simplicity, while providing also indoor-to-outdoor prediction and the achievement of a higher level of accuracy whenever a detailed 3D map of the building is available. Such accuracy level is found to be similar to that of ray tracing, but at a small fraction of the computation time.

When field prediction for indoor base stations or access points is needed both inside and "around" the building, such as for interference assessments and for fingerprinting localization purposes, the model can deliver it with good accuracy, as long as the actual base station location information is reasonably accurate.

ACKNOWLEDGEMENTS

The authors would like to thank Commscope Italy S.r.l. for having provided us with the indoor measurement equipment and helped us with the measurement campaigns.

REFERENCES

[1] *ESRI Shapefile Technical Description—An ESRI White Paper—July 1998*, accessed on Apr. 15, 2017. Available: https://www.esri.com/library/whitepapers/pdfs/shapefile.pdf

[2] *AutoCAD Architecture Features*, accessed on Apr. 15, 2017. Available: http://www.autodesk.com/products/autocad-architecture/overview

[3] A. Davidson and C. Hill, "Measurement of building penetration into medium buildings at 900 and 1500 MHz," *IEEE Trans. Veh. Technol.*, vol. 46, no. 1, pp. 161–168, Feb. 1997.

[4] H. Okamoto, K. Kitao, and S. Ichitsubo, "Outdoor-to-indoor propagation loss prediction in 800-MHz to 8-GHz band for an urban area," *IEEE Trans. Veh. Technol.*, vol. 58, no. 3, pp. 1059–1067, Mar. 2009.

[5] Y. Wang, S. Safavi-Naeini, and S. K. Chaudhuri, "A hybrid technique based on combining ray tracing and FDTD methods for site-specific modeling of indoor radio wave propagation," *IEEE Trans. Antennas Propag.*, vol. 48, no. 5, pp. 743–754, May 2000.

[6] F. Fuschini, M. Barbiroli, G. E. Corazza, V. Degli-Esposti, and G. Falciasecca, "Analysis of Outdoor-to-Indoor Propagation at 169 MHz for Smart Metering Applications," *IEEE Trans. Antennas Propag.*, vol. 63, no. 4, pp. 1811–1821, Apr. 2015.

[7] V. Kristem *et al.*, "3D MIMO outdoor to indoor macro/micro-cellular channel measurements and modeling," in *Proc. IEEE Global Commun. Conf. (GLOBECOM)*, San Diego, CA, USA, Dec. 2015, pp. 1–6.

[8] R. Wahl and G. Wolfle, "Combined urban and indoor network planning using the dominant path propagation model," in *Proc. 1st Eur. Conf. Antennas Propag. (EUCAP)*, Nice, France, Nov. 2006, pp. 1–6.

[9] A. Valcarce and J. Zhang, "Empirical indoor-to-outdoor propagation model for residential areas at 0.9–3.5 GHz," *IEEE Antennas Wireless Propag. Lett.*, vol. 9, no. 1, pp. 682–685, Jul. 2010.

[10] S. Hamid, A. J. Al-Dweik, M. Mirahmadi, K. Mubarak, and A. Shami, "Inside-out propagation: Developing a unified model for the interference in 5G networks," in *IEEE Veh. Technol. Mag.*, vol. 10, no. 2, pp. 47–54, Jun. 2015.

[11] D. Umansky, G. de la Roche, Z. Lai, G. Villemaud, J.-M. Gorce, and J. Zhang, "A new deterministic hybrid model for indoor-to-outdoor radio coverage prediction," in *Proc. 5th Eur. Conf. Antennas Propag. (EUCAP)*, Rome, Italy, Apr. 2011, pp. 3615–3618.

[12] D. M. Rose, T. Jansen, and T. Kürner, "Indoor to outdoor propagation—Measuring and modeling of femto cells in LTE networks at 800 and 2600 MHz," in *Proc. IEEE GLOBECOM Workshops (GC Wkshps)*, Houston, TX, USA, Dec. 2011, pp. 203–207.

[13] L. Shi and T. Wigren, "AECID fingerprinting positioning performance," in *Proc. IEEE Global Telecommun. Conf. (GLOBECOM)*, Honolulu, Hawaii, Nov. 2009, pp. 1–6.

[14] Y.-C. Cheng, Y. Chawathe, A. LaMarca, and J. Krumm, "Accuracy characterization for metropolitan-scale Wi-Fi localization," in *Proc. MOBISYS*, Seattle, WA, USA, Jun. 2005, pp. 233–245.

[15] J. M. Keenan and A. J. Motley, "Radio coverage in buildings," *Brit. Telecom Technol. J.*, vol. 8, no. 1, pp. 19–24, Jan. 1990.

[16] M. Lott and I. Forkel, "A multi-wall-and-floor model for indoor radio propagation," in *Proc. IEEE VTS 53rd Veh. Technol. Conf.*, vol. 1. Rhodes, Greece, May 2001, pp. 464–468.

[17] A. Durantini and D. Cassioli, "A multi-wall path loss model for indoor UWB propagation," in *Proc. IEEE 61st Veh. Technol. Conf.*, vol. 1. Stockholm, Sweden, May 2005, pp. 30–34.

[18] V. Degli-Esposti, G. Falciasecca, F. Fuschini, and E. M. Vitucci, "A Meaningful Indoor Path-Loss Formula," *IEEE Antennas Wireless Propag. Lett.*, vol. 12, no. 1, pp. 872–875, Jun. 2013.

[19] F. Fuschini, E. M. Vitucci, M. Barbiroli, G. Falciasecca, and V. Degli-Esposti, "Ray tracing propagation modeling for future small-cell and indoor applications: A review of current techniques," *Radio Sci.*, vol. 50, no. 6, pp. 469–485, Jun. 2015.

[20] R. A. Valenzuela, S. Fortune, and J. Ling, "Indoor propagation prediction accuracy and speed versus number of reflections in image-based 3-D ray-tracing," in *Proc. 48th IEEE Veh. Technol. Conf. (VTC)*, vol. 1. Ottawa, Canada, May 18-21, 1998, pp. 539–543.

[21] E. M. Vitucci, L. Tarlazzi, F. Fuschini, P. Faccin, and V. Degli-Esposti, "Interleaved-MIMO DAS for indoor radio coverage: Concept and performance assessment," *IEEE Trans. Antennas Propag.*, vol. 62, no. 6, pp. 3299–3309, Jun. 2014.

[22] L. Tarlazzi, P. Faccin, E. M. Vitucci, F. Fuschini, and V. Degli-Esposti, "Characterization of an Interleaved F-DAS MIMO indoor propagation channel," in *Proc. Loughborough Antennas Propag. Conf. (LAPC)*, Nov. 2010, pp. 505–508.

VITTORIO DEGLI-ESPOSTI (M'94–SM'16) received the Laurea degree (Hons.) and the Ph.D. degree in electronic engineering from the University of Bologna, Italy, in 1989 and 1994, respectively. Since 1994, he has been with the Department of Electrical Engineering, University of Bologna, where he is currently an Associate Professor and teaches courses on electromagnetics, radio propagation, and wireless systems.

From 2015 to 2016, he was on leave from his University position to join Polaris Wireless Inc., Mountain View, CA, USA in the role of the Director of Research.

He was a Visiting Researcher with Polytechnic University, Brooklyn, New York (now NYU Polytechnic) in the group led by Prof. H. L. Bertoni in 1998. He held visiting professor positions with Aalto University, in 2006, and Tongji University, Shanghai, in 2013, where he taught courses on deterministic propagation modeling and ray tracing.

He is currently a Co-Organizer and a Lecturer of the biennial Ph.D. Courses Short range radio propagation: theory, models and future applications and Large Scale Radio Propagation of the European School of Antennas.

He has participated in several European projects, including the European Cooperation Actions COST 231, 259, 273, 2100, and IC1004, the European Networks of Excellence NEWCOM and NEWCOM++ the 7th FP IP European Project ALPHA, and others.

He was appointed as a Vice-Chair of the European Conference on Antennas and Propagation (EuCAP), editions 2010 and 2011. He has been the Short-Courses and Workshops Chair of EuCAP 2015. He was an Elected Member of the Radio Propagation Board of the European Association on Antennas and Propagation from 2013 to 2015. In 2013, he has been the Elected Chair of the Cesena-Forli Unit of the Inter-Department Center for Industrial Research on ICT (CIRI-ICT), University of Bologna.

He has authored or co-authored over 110 peer-reviewed technical papers in the fields of applied electromagnetics, radio propagation, and wireless systems. He is an Associate Editor of the scientific Journal the IEEE Access.

ENRICO M. VITUCCI (S'04–M'08) received the M.Sc. degree in telecommunication engineering and the Ph.D. degree in electrical engineering from the University of Bologna, Italy, in 2003 and 2007, respectively. In 2007, he was a Visiting Researcher with Aalto University, Finland. From 2015 to 2016, he was a Visiting Researcher with Polaris Wireless, Inc., Mountain View, USA. He is currently a Post-Doctoral Fellow with the Center for Industrial Research on ICT (CIRI ICT), University of Bologna. He has authored or co-authored over 50 technical papers on international journals or conferences. His research interests are in mobile radio propagation, ray tracing models, MIMO channel modeling, solar radiation, and energy efficiency in urban areas. He participated in the European Cooperation Actions COST 2100, COST IC1004, COST CA15104, in the European Networks of Excellence FP6-NEWCOM and FP7-NEWCOM++, and in the EU Integrated Project FP7-ICT-ALPHA. He is a member of the Editorial Board of the journal *Wireless Communications and Mobile Computing*. He also serves as a Reviewer for a number of international conferences and journals, including several IEEE Transactions.

R. MARTIN, photograph and biography not available at the time of publication.